




Hierarchical Pigeon-Inspired Optimization-Based MPPT Method for Photovoltaic Systems Under Complex Partial Shading Conditions

Zhuoli Zhao , Member, IEEE, Mingyu Zhang, Zehan Zhang, Yuwu Wang , Runting Cheng, Juntao Guo, Ping Yang, Member, IEEE, Chun Sing Lai , Senior Member, IEEE, Peng Li, and Loi Lei Lai , Life Fellow, IEEE

Abstract—This article proposes a novel maximum power point tracking (MPPT) method based on the variant of the pigeon-inspired optimization (PIO) algorithm for photovoltaic systems under partial shading conditions (PSCs). The proposed method integrates the hierarchical network behavior of pigeon flock and revises the map and compass operator of the original PIO algorithm to improve optimization efficiency. In addition, the landmark operator is used to perform a small-scale search to achieve fast tracking. Based on the combination of these mechanisms and dual-mode dynamic tracking scheme, the proposed hierarchical pigeon-inspired optimization (HPIO) MPPT method has a powerful search ability to deal with PSCs. To verify the superiority of the proposed HPIO MPPT method, it is compared with other existing advanced MPPT methods in simulation and experiments. Compared with traditional MPPT techniques based on

artificial intelligence, the proposed HPIO MPPT method has a higher success rate in tracking GMPP and excellent tracking speed under PSCs. And the HPIO method also shows excellent performance under complex PSC with multiple clusters and load-variation conditions.

Index Terms—Hierarchical pigeon-inspired optimization, maximum power point tracking, partial shading conditions, photovoltaic (PV) systems.

I. INTRODUCTION

IN RECENT years, photovoltaic (PV) power generation has attracted more and more attention because of the advantages of low operating cost and environmental friendliness. Since the maximum power point (MPP) of PV system changes with environmental conditions, MPP tracking (MPPT) has become a challenging task. PV array is composed of diodes and panels connected in series and parallel. When uneven light is irradiated on the PV array, partial shading conditions (PSCs) are formed. Thus, the diode causes the power-voltage (P-V) curve to have multiple peaks, and the realization of MPPT faces significantly increased difficulty [1].

Traditional MPPT algorithms, including perturbation and observation (P&O) algorithm [2], incremental conductance (IC) algorithm [3], and hill-climbing (HC) algorithm [4], were improved that adapts to rapid changes in irradiation. Conventional MPPT algorithms developed in the past are only suitable for PV systems with a single peak under uniform sunlight conditions, and they cannot track GMPP under PSCs effectively. In recent years, the application of soft computing methods to solve the MPPT problem under PSCs has become a hot topic. In [5] and [6], the use of artificial neural networks (ANN) and fuzzy logic control (FLC) to successfully track GMPP under PSCs were reported. However, these methods require extensive experience and involve complex calculations, which are not conducive to practical applications. In [7], a novel maximum power point scanning (MPPS) technique was developed, which can be integrated into the online or offline tester. Kermadi *et al.* [8] adopted an intelligent mechanism to systematically schedule the MPPT

Manuscript received June 9, 2021; revised September 8, 2021 and November 7, 2021; accepted December 4, 2021. Date of publication December 29, 2021; date of current version May 2, 2022. This work was supported in part by the National Natural Science Foundation of China 51907031, in part by the Guangdong Basic and Applied Basic Research Foundation (Guangdong-Guangxi Joint Foundation) 2021A1515410009, and in part by the Brunel Research Initiative and Enterprise Fund. (Corresponding authors: Chun Sing Lai; Loi Lei Lai.)

Zhuoli Zhao, Mingyu Zhang, Zehan Zhang, Runting Cheng, Juntao Guo, and Loi Lei Lai are with the Department of Electrical Engineering, School of Automation, Guangdong University of Technology, Guangzhou 510006, China (e-mail: zhuoli.zhao@gdut.edu.cn; mingyu@mail2.gdut.edu.cn; gdut3119001299@mail2.gdut.edu.cn; chengrunting@mail2.gdut.edu.cn; 2111904003@mail2.gdut.edu.cn; l.l.lai@ieee.org).

Chun Sing Lai is with the Department of Electrical Engineering, School of Automation, Guangdong University of Technology, Guangzhou 510006, China, and also with the Brunel Interdisciplinary Power Systems Research Centre, Department of Electronic & Electrical Engineering, Brunel University London, London, UB8 3PH, U.K. (e-mail: chun-sing.lai@brunel.ac.uk).

Yuwu Wang is with the School of Electric and Information Engineering, Guangxi University of Science and Technology, Liuzhou 545006, China (e-mail: wangyuwu@gxust.edu.cn).

Ping Yang is with the Guangdong Key Laboratory of Clean Energy Technology, South China University of Technology, Guangzhou 510640, China (e-mail: eppyang@scut.edu.cn).

Peng Li is with the Digital Grid Research Institute of China Southern Power Grid, Guangzhou 510663, China (e-mail: lipeng@csg.cn).

Color versions of one or more figures in this article are available at <https://doi.org/10.1109/TIE.2021.3137595>.

Digital Object Identifier 10.1109/TIE.2021.3137595

process, and used a novel skipping scheme to further minimize the search region.

Bioinspired algorithms are a new and important branch in the field of artificial intelligence (AI), which can well solve nonlinear and stochastic optimization problems and effectively improve the reliability of practical applications. Bioinspired algorithms have two main categories: evolutionary algorithms and algorithms based on swarm intelligence. Typical evolutionary algorithms combined with MPPT applications are genetic algorithm (GA) [9] and differential evolution (DE) [10]. Messai *et al.* [11] used GA to obtain the best member functions and control rules for FLC to improve the MPPT performance. Tey *et al.* [12] further improved the MPPT method based on DE, which can search for GMPP in a larger working area, thereby improving the ability to track GMPP.

In recent years, many swarm intelligence (SI) algorithms have been developed and applied to achieve MPPT for PV systems. A hybrid MPPT method combined the adaptive P&O and particle swarm optimization (PSO), which is proposed in [13], proved that it has a real global tracking effect with short tracking time. Seyedmahmoudian *et al.* [14] developed a novel method called adaptive radial movement optimization, which can maximize convergence speed and output fluctuation during tracking. In [15], a hybrid MPPT method combining adaptive neuro-fuzzy in reference system and particle swarm optimization was applied, which can track the MPP rapidly with zero oscillation. Singh *et al.* [16] developed a novel MPPT algorithm based on flying squirrel search optimization, which showed a higher convergence speed and performed better than P&O algorithm and PSO algorithm. Pillai *et al.* [17] proposed a hybrid tracking technology, which can switch between traditional P&O and flower pollination algorithm by accurately detecting shading conditions. Huang *et al.* [18] used improved fusion firefly algorithm to track the GMPP under PSCs, which integrated the neighborhood attraction firefly algorithm and simplified firefly algorithm, and achieved a high efficiency to track the GMPP. Makhloufi and Mekhilef [19] presented a logarithmic PSO method, which reduced the power oscillation during the MPPT process and accelerated the convergence. In [20], a modified butterfly optimization algorithm was developed to solve the MPPT problem under PSCs, which distinguished different partial shadow conditions with fast convergence speed.

The abovementioned studies have shown that various bioinspired AI-based algorithms have better performance than traditional MPPT algorithms such as P&O, IC, and HC, with higher tracking accuracy and faster tracking response. However, the selection of parameters and initial values has a great impact on the tracking performance of bio-inspired AI-based algorithms [21]. Inappropriate parameters and initial values may lead to local MPP (LMPP) or too long tracking time. Therefore, when designing parameters and initial values, it is necessary to find a balance between the three indicators of tracking success rate, tracking efficiency, and tracking speed.

Inspired by the behavior of homing pigeons in navigation, Duan and Qiao [22] proposed pigeon-inspired optimization (PIO) in 2014, which is a new SI algorithm. Pigeons can perceive the earth's magnetic field and use the sun as a compass to

generate a map in their brains to convert the direction, which is relative to the sun, into the actual flight direction. At the same time, pigeons have the memory to distinguish familiar landmarks, so that they can reach their destination fast and accurately. PIO is built on the abovementioned biological basis. In applications of unmanned aerial vehicle, PIO shows excellent performance with good convergence and high efficiency [23]. However, similar to other bioinspired algorithms, PIO still has the general problem of premature convergence [24].

Motivated by the aforementioned research gap, this article improves the PIO algorithm, and proposes a hierarchical network in the flock of pigeons to revise the map and compass operator, so as to improve the optimization efficiency. Moreover, the landmark operator also ensures fast convergence to achieve fast tracking speed. Therefore, the proposed hierarchical pigeon-inspired optimization (HPIO) method can quickly and efficiently track GMPP under various PSCs. On the basis of previous improvement, a tracking technique that switches between the HPIO and P&O algorithm in two modes is proposed. Simulations are carried out under 56 PSCs, and experiments are conducted for several cases. By comparing the other three existing advanced MPPT methods, the superiority of the proposed MPPT method is verified. The proposed MPPT method, which can switch between two MPPT modes, can be directly applied in actual operation and has good practicability. The contributions of this article are listed as follows.

- 1) Based on the research of hierarchical group dynamics in pigeon flock, a hierarchical network is constructed to revise map and compass operator of the original PIO algorithm, thus enhancing the global search ability and improving the tracking efficiency to track GMPP under PSCs.
- 2) A dual-mode dynamic tracking technique that switches between two MPPT modes is proposed. "Intelligent Mode" quickly determines the approximate position of GMPP, while "Disturbance Mode" maintains efficient dynamic tracking.
- 3) The proposed HPIO method is compared with other MPPT methods in specific cases and dynamic tracking tests with verification results. Tests under complex PSC with multiple clusters and tests under load-variation are also conducted to verify the effectiveness of the proposed method.

II. MODELING OF PV ARRAY AND CHARACTERISTICS UNDER PSCS

Assuming that the number of series and parallel are N_s and N_p , respectively, the I-V characteristics of the PV panel are [25]

$$I = N_p I_{pv} - N_p I_0 \left[\exp \left(\frac{qV + qR_s I N_s / N_p}{N_s k_s T a} - 1 \right) \right] - \frac{V N_p / N_s + R_s I}{R_p} \quad (1)$$

PV array is formed by connecting multiple PV panels in parallel or series, as shown in Fig. 1. The PV panel shaded under PSCs will cause the hot spot effect. To prevent damage to the

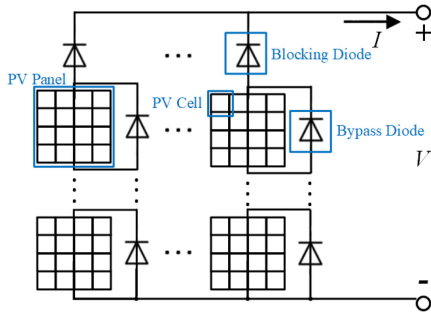


Fig. 1. Equivalent model of PV array.

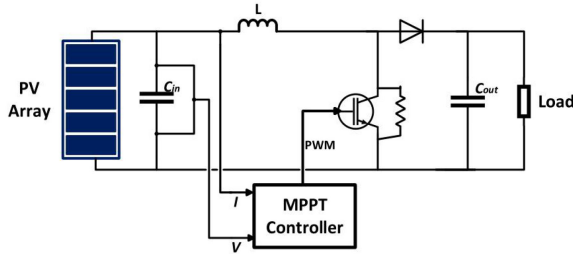


Fig. 2. Block diagram of the studied PV system.

 TABLE I
IRRADIANCE VALUES OF FOUR CASES

Cases	Irradiance Values of PV panels(W/m ²)					P_{max}
	Panel 1	Panel 2	Panel 3	Panel 4	Panel 5	
Case 1	1000	1000	1000	1000	1000	498.4W
Case 2	1000	875	750	625	500	294.4W
Case 3	1000	875	750	625	375	281.9W
Case 4	1000	875	375	250	125	172.9W

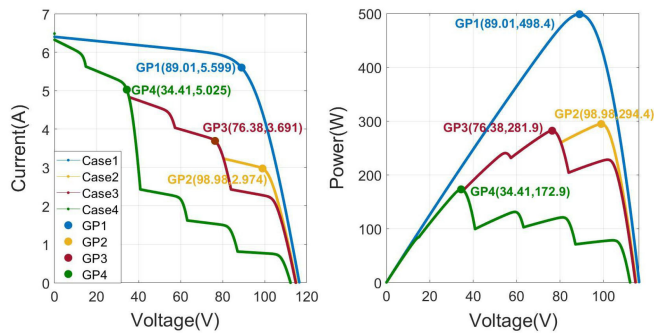


Fig. 3. I-V and P-V characteristic curves of PV arrays under four cases.

PV panel due to overheating, it is necessary to connect a bypass diode to the PV panel in parallel. However, due to the conduction of the diode, the output characteristics of the PV array under PSCs will have multiple extreme points, and this phenomenon is obvious in a PV array composed of multiple PV panels in series.

Fig. 2 shows the studied PV system, and the PV array consists of five modules connected in series. Table I shows the different irradiance combinations for the four GMPP locations. Fig. 3 shows the I-V and P-V characteristic curves of the four cases. In Case 1, the PV array receives the same radiance. Among the

other three PSCs, the five PV panels of the PV array receive five different irradiances, and there are five MPPs on the P-V characteristic curve, but the location of GMPP is different. In Case 2, GMPP is located at GP2 near 85% Voc. In Case 3, GMPP is located at GP3 near 30% Voc. In Case 4, GMPP is located at GP4 near 65% Voc.

III. PROPOSED METHOD

A. Principle of PIO Algorithm

Homing pigeons have played a significant role in transmitting information in human history. Studies have found that the excellent homing ability of pigeons depends on the ability to use the geomagnetic field and the sun to determine the direction, which play the role of “map and compass” [22]. As the pigeon approaches the destination, the navigational role of the “map and compass” gradually weakens, and the navigation tools are eventually replaced with landmarks [26]. Inspired by the behaviors in homing pigeon navigation, Duan and Qiao [22] proposed pigeon-inspired optimization. This novel bioinspired intelligence algorithm includes two operators: map and compass operator, landmark operator. The former emphasizes the influence of the sun and the geomagnetic field on navigation, while the latter emphasizes the influence of landmarks. The process of the PIO algorithm can be divided into two parts.

1) Map and Compass Operator: In multidimensional search space, the position and speed of the pigeons are initialized and will be updated in each iteration. Its position and speed are denoted as x_i and v_i ($i = 1, 2, \dots, N$). During each iteration, the pigeon flies toward the global optimal position and maintains a certain speed inertia, which makes the PIO algorithm have an excellent global search capability. Each pigeon updates its position x_i and speed v_i by

$$v_i^k = v_i^{k-1} \cdot e^{-R \cdot k} + rand \cdot (x_{gbest} - x_i^{k-1}) \quad (2)$$

$$x_i^k = x_i^{k-1} + v_i^k \quad (3)$$

where R is the map and compass factor, the value range is set to 0–1; $rand$ is a random number with a value range of 0–1; k is the current iteration number; x_{gbest} is the global optimal position obtained after $k-1$ iteration loops.

2) Landmark Operator: When approaching the destination, the pigeons will rely on nearby landmarks to optimize their position. The pigeons, which are familiar with the landmark will fly directly to the destination, while other pigeons that are not familiar with the landmark will follow the former. According to the principle of the landmark operator, the number of pigeons will be reduced by half after each iteration. x_{center} is the center position of the remaining pigeons and will be used as a landmark. Therefore, x_i is updated according to

$$N^k = \frac{N^{k-1}}{2} \quad (4)$$

$$x_{center}^k = \frac{\sum_{i=1}^{N^k} x_i^{k-1} \cdot F_i^{k-1}}{N^k \cdot \sum_{i=1}^{N^k} F_i^{k-1}} \quad (5)$$

$$x_i^k = x_i^{k-1} + rand \cdot (x_{center}^k - x_i^{k-1}) \quad (6)$$

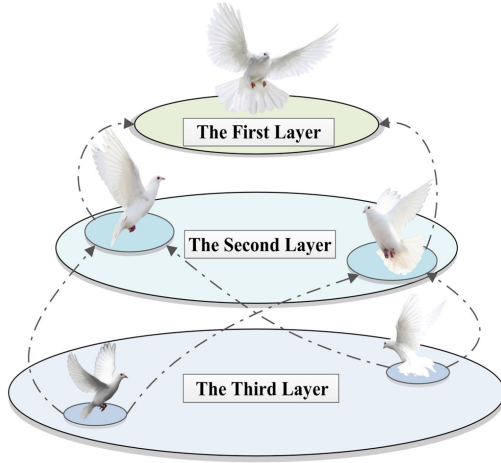


Fig. 4. Conceptual diagram of the hierarchical network of pigeon flocks.

$$F_i^{k-1} = \begin{cases} \frac{1}{\text{Fitness}(x_i^{k-1}) + \varepsilon}, & \text{for minimization} \\ \text{Fitness}(x_i^{k-1}), & \text{for maximization} \end{cases} \quad (7)$$

where ε is a constant close to zero to ensure the validity of the equation. When the landmark operator stops, the PIO ends the iteration and obtains the historical global optimal position x_p .

B. Proposed Hierarchical PIO

Analyzing the map and the compass operator, it can be found that the conventional PIO algorithm is easy to fall into the local extreme value. In the early stage of the PIO algorithm, it is hoped to have a strong global search capability, so as to keep away from converging prematurely. To further improve the optimization efficiency of the PIO algorithm and prevent it from falling into a local optimal solution, this article proposes the Hierarchical PIO Algorithm. This design is inspired by the implicit hierarchical network in the pigeon flock proposed by Nagy *et al.* in *Nature* [27], in which the relationship between leaders and followers is consistently manifested. In addition, Nagy *et al.* [28] also showed that there is a hierarchical network of directional interaction in the pigeon flock, and the individual quality of the pigeon can be used as a predictor to maintain a dominant position in the group structure.

In the proposed HPIO algorithm, the hierarchical network consists of three layers. The first layer is considered to be the leaders of the pigeons of the second layer. The same is true for the relationship between the second and third layers. By letting followers imitate the leader's movement, the pigeon flock's movement decisions can be better optimized. Fig. 4 shows the conceptual diagram of the hierarchical network of pigeon flocks.

1) Revised Map and Compass Operator: Initialize the position and velocity of the pigeon flock with the population size of N , and the population size of each layer from the first to the third layer is denoted as N_1, N_2, N_3 . The research in [27] reveals that most individuals in the bird flock tend to assume leadership roles, and the level of leadership is likely

to be related to individual navigation efficiency. In the proposed HPIO algorithm, before updating the position in each iteration, the pigeon flock is relayered according to the ranking of the individual fitness function values

$$\text{rank}(x_1, x_2, \dots, x_N) = [x_{\text{rank } 1}, x_{\text{rank } 2}, \dots, x_{\text{rank } N}] \quad (8)$$

$$\text{rank}(x_1, x_2, \dots, x_N) = [v_{\text{rank } 1}, v_{\text{rank } 2}, \dots, v_{\text{rank } N}]. \quad (9)$$

Thus, the position and velocity of each pigeon sorted according to the individual fitness value from large to small are obtained. They are denoted as $x_{\text{rank } j}$ and $v_{\text{rank } j}$. In the process of updating the position in each iteration, the pigeon of the first layer, considered the current highest leader, flies to the historical optimal position, and other followers fly to the position where their leaders were before the update. Under this hierarchical network, all pigeons make new motion decisions at the same time, and there is no time delay in information transmission between individuals at different layers. The revised map and compass operators in the HPIO algorithm are expressed as

While $j = 1, \dots, N_1$

$$v_{\text{rank } j}^k = v_{\text{rank } j}^{k-1} \cdot e^{-R \cdot k} + \text{rand} \cdot (x_{g\text{best}} - x_{\text{rank } j}^{k-1}). \quad (10)$$

While $j = N_1 + 1, \dots, N_1 + N_2$

$$v_{\text{rank } j}^k = v_{\text{rank } j}^{k-1} \cdot e^{-R \cdot k} + \sum_{m=1}^{N_1} \text{rand} \cdot (x_{\text{rank } m}^{k-1} - x_{\text{rank } j}^{k-1}). \quad (11)$$

While $j = N_1 + N_2 + 1, \dots, N$

$$\begin{aligned} v_{\text{rank } j}^k \\ = v_{\text{rank } j}^{k-1} \cdot e^{-R \cdot k} + \sum_{m=N_1+1}^{N_1+N_2} \text{rand} \cdot (x_{\text{rank } m}^{k-1} - x_{\text{rank } j}^{k-1}). \end{aligned} \quad (12)$$

Compared with the conventional PIO algorithm, in this operator, all the pigeons in the pigeon flock do not directly fly to the historical optimal position, but fly to different positions hierarchically. This makes the search scope further increase, so the HPIO algorithm has a stronger global search capability.

In the stage of the revised map and compass operator, this article proposes a convergence judgment method based on the degree of clustering of pigeons. Denote the position distribution width of the pigeon group as α , the convergence condition is

$$\alpha^k < A \quad (13)$$

where A is the convergence factor. When (13) is satisfied, end the optimization of the current stage and enter the landmark operator.

2) Consistent Landmark Operator: When approaching the destination, the pigeon tends to use landmarks as the navigation tool. In this operator, the number of pigeons is reduced by half after each iteration, and the remaining pigeons fly to the

center position x_{center} . The contribution of the landmark operator makes the HPIO algorithm has a strong local search ability in the later stage while having a powerful global search ability in the early stage. In this article, the convergence condition of the landmark operator stage is defined as

$$N^k = 1. \quad (14)$$

When (14) is satisfied, obtain the historical global best position $x_{g\text{best}}$, and the process of the proposed algorithm is completed.

3) HPIO-Based MPPT Method

When the proposed MPPT method is applied, the position of the pigeon is expressed as duty cycle D , and the fitness function is expressed as power P .

To use HPIO for designing MPPT, we need to determine the control variable, objective function, and constraints for the optimization process. First, the control variable is chosen as the duty cycle D . Second, the objective function is $\max(P_j^k)$. Third, the constraints include: $D_{\min} \leq D_j^k \leq D_{\max}$ (D_{\max} and D_{\min} are chosen as 0.90 and 0.10, respectively), the maximum number of duty cycle changes is 50.

The process of the method is as follows.

Step 1: Set the initial population number $N = 5$, the number of pigeons in the first layer $N_1 = 1$, the number of pigeons in the second layer $N_2 = 2$, and the number of pigeons in the third layer $N_3 = 2$. The duty cycle of pigeons is initialized with uniform distribution.

Step 2: Output the duty cycle of all pigeons, measure the voltage and current of the PV system, and then calculate the power of each pigeon. Compare them with the previous historical global optimal power $P_{g\text{best}}$ obtained, and update the historical global optimal duty cycle $D_{gb} = x_{g\text{best}}$. Set $k = k + 1$.

Step 3: Sort the pigeons by comparing the power values from large to small, thus establishing a top-down hierarchical network.

Step 4: Implement the revised map and compass operator, and use the optimization mechanism of the hierarchical network to update the duty cycle and velocity of pigeons.

Step 5: Check the first convergence condition: if the position distribution width of the pigeon flock α^k satisfies (13), jump to Step 6; otherwise, return to Step 2.

Step 6: Use the same content as in Step 2.

Step 7: Implement the landmark operator: update N^k , the center duty cycle $D_{\text{center}}^k = x_{\text{center}}^k$ and the duty cycle of the remaining pigeons.

Step 8: If the number of remaining pigeons N^k satisfies (14), skip to Step 9; otherwise, return to Step 6.

Step 9: End and output the historical global optimal duty cycle D_{gb} .

Furthermore, a tracking technique is introduced, which switches between two MPPT modes. At the initial startup, the HPIO algorithm is activated to quickly determine the approximate location of GMPP, this process is called ‘‘Intelligent Mode’’; then activate the P&O algorithm, so that the real-time

tracking point is disturbed near the GMPP, this process is called ‘‘Disturbance Mode’’. The ‘‘Intelligent Mode’’ can be reactivated when the irradiance changes are detected with the following condition:

$$\Delta P\% = |(P^k - P^{k-1})/P^k| > 2\% \quad (15)$$

where P^k and P^{k-1} represent the power values corresponding to the two adjacent duty cycles.

The flowchart of the proposed method is shown in Fig. 5. Fig. 6 shows the position changes of the pigeon flock during a single tracking process.

Iteration 1: Sends five initial positions of pigeons and samples the voltage and current of the PV array to calculate the corresponding power of each duty cycle. In this iteration, D_3 is D_{gb} .

Iteration 2: Execute revised map and compass operator of HPIO algorithm to obtain the second generation of pigeons. In this iteration, D_3 is the optimal position among the five positions again, and the position of D_3 is the same as the previous iteration.

Iteration 3: Repeat *Iteration 2* and obtain the third generation of pigeons. D_4 is the current optimal position among the five positions. Since $P(D_4) > P(D_{gb})$, D_{gb} is replaced by D_4 .

Iteration 4: Repeat the same process as the last iteration and obtain the fourth generation. D_3 is the current optimal position. Since $P(D_3) = P(D_{gb})$, D_{gb} remains unchanged.

Iteration 5: Repeat the same process as the last iteration and obtain the fifth generation. D_2 is the current optimal position. Due to $P(D_2) = P(D_{gb})$, D_{gb} remains unchanged. After this iteration, (13) is satisfied. Thus, the landmark operator will be executed in the following iteration.

Iteration 6: Execute the landmark operator of HPIO to obtain the sixth generation. Two pigeons with the worst positions in the previous iteration will be discarded, and the remaining three pigeons will be given new positions. By comparison, D_2 is the current optimal position. Due to $P(D_2) > P(D_{gb})$, D_{gb} is replaced by D_2 .

Iteration 7: In this iteration, D_5 will be discarded, D_2 and D_3 will move toward the center of themselves. Since D_2 and D_3 are almost coincident in *Iteration 6*, D_{gb} will not change after *Iteration 7*. Since the change process of *Iteration 7* is not obvious, the process of *Iteration 7* is not drawn in Fig. 6.

After *Iteration 7*, by continuing to execute the landmark operator, the number of pigeons N is reduced to one. And the convergence condition in (14) is satisfied. Thus, the iterative process of the HPIO stops and D_{gb} outputs as the historical global best. At this point, the HPIO algorithm has been completed.

IV. SIMULATION RESULTS

To verify the effectiveness of the proposed HPIO-based MPPT method, a 500 W PV system is built, as shown in Fig. 2. The PV module is FG-2BTM-100, with the parameters shown in Table II. The parameters of circuit components are listed in Table III. The simulation studies are implemented under MATLAB/Simulink.

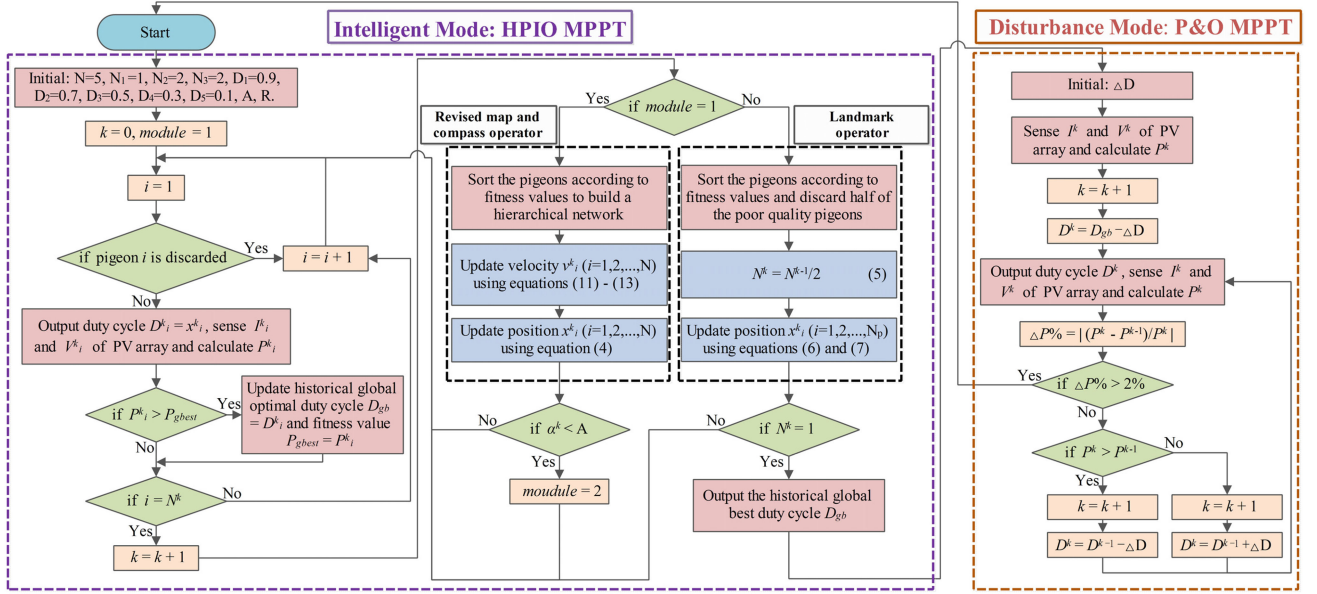


Fig. 5. Flowchart of the proposed MPPT method combined with HPIO and P&O MPPT algorithms.

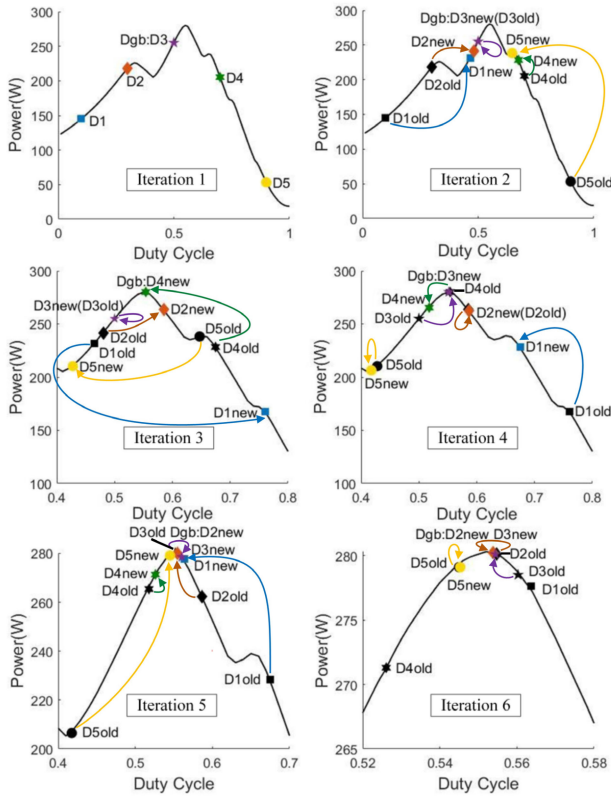


Fig. 6. Position changes of the pigeon flock during a single tracking process.

The performance of the proposed HPIO method is compared with original PIO algorithm and four existing advanced MPPT techniques, including deterministic particle swarm optimization (DPSO) in [29], modified firefly algorithm (MFA) in [30], overall distribution (OD) in [21], cubic-spline-guided Jaya (S-Jaya)

TABLE II
PARAMETERS OF THE PV MODULE

PV module data	FG-2BTM-100	5S1P System
Maximum Power P_{max}	99.68 W	498.4 W
Open circuit voltage V_{oc}	23.3 V	116.5 V
Short-circuit current I_{sc}	6.4 A	6.4 A
Voltage at maximum power point V_{mpp}	17.8 V	89 V
Current at maximum power point I_{mpp}	5.6 A	5.6 A
Temperature coefficient of V_{oc}	-0.32601 (%/deg.C)	-0.35691 (%/deg.C)
Temperature coefficient of I_{sc}	0.006 (%/deg.C)	0.050102 (%/deg.C)

TABLE III
PARAMETERS OF CIRCUIT COMPONENTS

Specification	Parameter
Input Voltage at maximum power point (V_{in})	89 V
Output Voltage at maximum power point (V_{out})	223 V
Output Power of PV array at maximum power point (P_{out})	498.4 W
Switching Frequency (f_s)	20 kHz
L	2 mH
C_{in}	1 μ F
C_{out}	10 μ F

in [31]. In addition, in order to show the comparison between the proposed method and the non-artificial intelligence-based method, modified incremental conductance (MIC) in [32] is selected as the last comparison algorithm. In order to analyze the capability of different MPPT methods to deal with PSCs, it is necessary to set up multiple combinations of irradiance for simulation. The full sunshine condition is defined as receiving $G_0 = 1000 \text{ W/m}^2$, while the partial shading conditions receive $G_i = n_i \times G_0 \text{ W/m}^2$ ($n_i \times 100\%$ of the full sunshine). Thus, the irradiance value of each PV module is $n_i \times 1000$ ($n_i \in \{0.125, 0.250, 0.375, 0.500, 0.625, 0.750, 0.875, 1.000\}$). Based on the abovementioned analysis, 56 (C_8^5) PSCs can be obtained. The

average performances of the seven MPPT methods are obtained by combining the simulation results under 56 PSCs.

A. Performance Evaluation

To accurately evaluate the performance, the performance of the MPPT methods is compared through three indicators as follows.

1) Static Tracking Efficiency η

$$\eta = \frac{P_m}{P_{MPP}} \times 100\% \quad (16)$$

where P_m is the final maximum output power, and P_{MPP} is the theoretical value of the maximum output power.

2) Tracking Time T

T is defined as the time for the PV system to reach a stable output. It can be measured by the number of sampling cycles.

3) Tracking Success Rate σ

$$\sigma = \frac{N_{st}}{N_s} \times 100\% \quad (17)$$

where N_{st} is the number of successful tracking times, and N_s is the number of simulated times.

The condition for judging the tracking success of the MPPT method is successfully tracking the peak where the GMPP is located and meets the following conditions:

$$\eta \geq 95\% \quad (18)$$

$$\frac{|V_m - V_{MPP}|}{V_{MPP}} \leq 0.03 \quad (19)$$

where V_m is the final output voltage of the PV system, and V_{MPP} is the theoretical value of the output voltage at MPP.

4) Dynamic Tracking Efficiency η_d

$$\eta_d = \frac{P_{ave}}{P_{MPP}} \times 100\% \quad (20)$$

where P_{ave} is defined as the average output power of the PV system using the MPPT algorithm for a period of T_{ave} seconds after starting the MPPT algorithm. In this article, T_{ave} is selected as 0.6 s.

B. Determination of Parameters for HPIO

It can be seen from (10)–(12) that the value of R needs to be determined for the proposed method. In this article, R is determined based on a large number of simulation results. First, based on preliminary simulation tests, it can be found that when the value of R is in the range of 0.40 to 0.85, the proposed HPIO method can realize MPPT with good results. To further determine the optimal value of R , R is set to 10 values (0.40, 0.45, 0.50, 0.55, 0.60, 0.65, 0.70, 0.75, 0.80, 0.85), and ten HPIO methods with these different R values are tested under 56 PSCs. Table IV shows the average performances of ten HPIO methods with different R under 56 PSCs. It can be seen that as the value of R increases, the tracking time gradually shortens. When the value of R is 0.60, the proposed HPIO method obtains the optimal tracking success rate and tracking efficiency. Based

TABLE IV
SIMULATION RESULTS OF THE PROPOSED HPIO METHOD WITH DIFFERENT VALUES OF R

MPPT method	Parameter	Tracking time T (s)	Tracking efficiency η (%)	Tracking success rate σ
The proposed HPIO method	$R = 0.40$	0.3184	98.67	89.29% (50/56)
	$R = 0.45$	0.3107	98.63	89.29% (50/56)
	$R = 0.50$	0.3080	98.60	89.29% (50/56)
	$R = 0.55$	0.2938	98.84	92.86% (52/56)
	$R = 0.60$	0.2946	99.20	100.0% (56/56)
	$R = 0.65$	0.2932	98.92	96.43% (54/56)
	$R = 0.70$	0.2896	98.78	96.43% (54/56)
	$R = 0.75$	0.2875	98.92	92.86% (52/56)
	$R = 0.80$	0.2886	98.84	92.86% (52/56)
	$R = 0.85$	0.2864	98.57	85.71% (48/56)

on the abovementioned analysis, the value of R is finally selected as 0.60.

In the proposed HPIO MPPT method, the selection of parameter A needs to be adjusted according to the number N_s of series connected modules. In order to ensure that the flock of pigeons has gathered on the peak where the GMPP is located when the first convergence condition is met, the setting formula of A is proposed in this article, namely

$$A < 0.5 \frac{1}{N_s}. \quad (21)$$

The coefficient “0.5” is set to ensure that “ A ” can be used as the duty cycle distribution width to determine the first stage of convergence. Therefore, the value of A should be set as 0.10.

C. Comparative Simulated Results Under 56 PSCs

Table V shows the parameters of the seven MPPT methods and the average performance results under 56 PSCs. ε represents the convergence threshold of the three MPPT methods for comparison. When the difference between all duty cycles is less than ε , the MPPT algorithm ends and outputs the global best duty cycle D_{gb} . It can be seen that the DPSO method has a slow convergence speed and exhibits the lowest dynamic tracking efficiency. However, it has a strong shadow tracking ability to achieve successful tracking. The MFA method is easy to obtain a solution prematurely, thus, its ability to deal with shadows is weak and easily leads to tracking failure. The OD method can complete the tracking process in a shorter time compared with the DPSO method, and it has a high tracking success rate while its dynamic performance is also better. The S-Jaya method shows good dynamic tracking performance. However, its static tracking efficiency is not well, and does not well achieve the requirement of accurate tracking to GMPP. Different from the abovementioned swarm-intelligence-based algorithm, the MIC method realizes intelligent scanning to the PV characteristic curve by using the relevant parameters of the PV array. Since its principle of tracking is based on the scanning method, it takes a long tracking time and has poor dynamic performance, but it has a high tracking success rate. Compared with the S-Jaya method, the original PIO method takes shorter tracking time and has a more comprehensive tracking performance. But compared with

TABLE V
SIMULATION RESULTS OF SEVEN MPPT METHODS UNDER 56 PSCs

MPPT methods	Parameter	Tracking time T (s)	Static Tracking efficiency η	Tracking success rate σ	Dynamic tracking efficiency η_d
The proposed HPIO method	$N = 5$ $N_1 = 1$ $N_2 = 2$ $N_3 = 2$ $R = 0.6$ $A = 0.1$	0.2946	99.20%	100.0% (56/56)	93.42%
The DPSO method in [29]	$N = 3$ $\omega = 0.4$ $V_{max} = 0.035$ $\varepsilon = 0.07$	0.4745	99.30%	98.21% (55/56)	84.80%
The MFA method in [30]	$N = 5$ $\beta_0 = 1$ $\gamma = 0.96$ $\varepsilon = 0.05$	0.1855	98.07%	83.93% (47/56)	93.06%
The OD method in [21]	$N = 5$ $\gamma = 0.1$ $\varepsilon = 0.07$	0.3988	99.31%	96.43% (54/56)	89.06%
The S-Jaya method in [31]	$N=5$	0.3438	98.30%	94.64% (53/56)	91.20%
The MIC method in [32]	$\Delta D = 0.015$ $V_{oc} = 23.3$ $V_{max} = 116.5$ $V_{min} = 0$ $N_{max} = 5$	0.4408	99.29%	100.0% (56/56)	86.65%
The original PIO method	$N=5$ $R=0.6$ $A=0.1$	0.3034	99.08%	94.64% (53/56)	92.77%

OD, DPSO, and MIC methods, this method still has room for improvement in static tracking efficiency. Compared with the four advanced AI-based and one non-AI-based MPPT techniques above and the original PIO method, the proposed HPIO method has the highest tracking success rate, reaching 100%, and has the highest dynamic tracking efficiency. Compared with the original PIO method, the tracking performance of the proposed method has overall been further improved. Furthermore, the proposed HPIO method has a fast convergence speed, second only to the MFA method.

Although the static tracking efficiency of the proposed HPIO method is slightly lower than that of the OD, DPSO, and MIC methods, due to its powerful shadow tracking ability, superior dynamic tracking efficiency, and fast convergence speed, the proposed HPIO method exhibits the most superior comprehensive tracking performance among the seven MPPT methods. The proposed HPIO method can achieve superior tracking results in a shorter T time and then output the historical optimal power point. According to the MPPT process proposed in this article, the abovementioned seven MPPT methods are implemented in the first mode—"Intelligent Mode". Next, the PV system enters the second mode—"Disturbance Mode". With the regular disturbance of the duty cycle near the GMPP position, it continues to obtain higher tracking efficiency. The abovementioned analysis shows that the proposed HPIO method has excellent performances in dealing with complex PSCs.

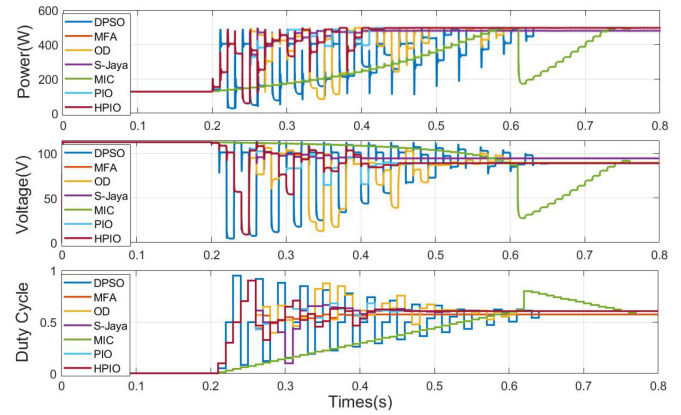


Fig. 7. Output waveforms during the tracking process in Case 1.

D. Specific Cases Analysis

Next, Table VI shows the simulation results of the seven MPPT methods under four different cases given in Table I and Fig. 3. Later, we also give the results of the dynamic tracking test.

- 1) *Case 1*: The output waveforms during the tracking process of the seven MPPT methods are shown in Fig. 7. It can be observed that the proposed HPIO method completes tracking within 0.25 s, and the static tracking efficiency reaches 99.48%; and the dynamic tracking efficiency reaches 91.01%, the highest among the seven MPPT methods. The DPSO, MIC, S-Jaya, and original PIO method complete the tracking within 0.45, 0.56, 0.35, and 0.3 s, respectively. Their static tracking efficiency also reach 99.48%. The MFA method only takes 0.2 s to complete the tracking, but does not track to the location near GMPP, the static tracking efficiency is only 96.15%. The OD method completes the tracking within 0.4 s, and the static tracking efficiency reaches 99.46%. Due to the long tracking time, DPSO, OD, and MIC methods show a low dynamic tracking efficiency while the dynamic tracking efficiency of the other four methods all reach more than 90%. Though the MFA method has the fastest tracking speed, it fails to track GMPP in this case, indicating that the MFA method lacks certain search ability.
- 2) *Case 2*: It can be seen from Fig. 8 that the HPIO, DPSO, MFA, OD, MIC, and original PIO methods complete the tracking within 0.3, 0.45, 0.2, 0.4, 0.45, and 0.3 s, respectively, and the six MPPT methods finally achieve the same static tracking efficiency of 99.21%. The S-Jaya method completes the tracking within 0.35 s, and the static tracking efficiency only reaches 98.02%. In this case, the MFA method shows the highest dynamic tracking efficiency of 95.62%; the HPIO method is second only with 93.45%; the dynamic tracking efficiency of MPPT methods except DPSO and MIC reach more than 90%. Obviously, the proposed HPIO method shows the tracking speed and dynamic tracking efficiency second only to the MFA method, and its static tracking efficiency is no less than that of the other six MPPT methods.

TABLE VI
SIMULATION RESULTS OF SEVEN MPPT METHODS UNDER FOUR CASES

Cases	MPPT method	Tracking voltage (V)	Tracking power (W)	Tracking time T (s)	Static Tracking efficiency η (%)	Dynamic Tracking efficiency η_d (%)	Tracking GMPP success?
Case 1	The proposed HPIO method	88.88	495.8	0.25	99.48	91.01	Yes
	The DPSO method in [29]	88.88	495.8	0.45	99.48	75.15	Yes
	The MFA method in [30]	94.41	479.2	0.20	96.15	90.60	No
	The OD method in [21]	89.31	495.7	0.40	99.46	85.78	Yes
	The S-Jaya method in [31]	88.43	495.8	0.35	99.48	90.31	Yes
	The MIC method in [32]	88.88	495.8	0.56	99.48	80.94	Yes
	The original PIO method	88.88	495.8	0.30	99.48	90.55	Yes
Case 2	The proposed HPIO method	98.23	292.1	0.30	99.21	93.45	Yes
	The DPSO method in [29]	98.23	292.1	0.45	99.21	82.47	Yes
	The MFA method in [30]	98.56	292.1	0.20	99.21	95.62	Yes
	The OD method in [21]	98.56	292.1	0.40	99.21	91.68	Yes
	The S-Jaya method in [31]	100.40	288.6	0.35	98.02	90.30	Yes
	The MIC method in [32]	98.56	292.1	0.45	99.21	78.20	Yes
	The original PIO method	98.23	292.1	0.30	99.21	92.62	Yes
Case 3	The proposed HPIO method	75.73	280.2	0.30	99.38	92.87	Yes
	The DPSO method in [29]	76.06	280.1	0.42	99.35	82.27	Yes
	The MFA method in [30]	75.38	280.1	0.20	99.35	94.67	Yes
	The OD method in [21]	75.38	280.1	0.40	99.35	89.08	Yes
	The S-Jaya method in [31]	75.73	280.2	0.35	99.38	91.72	Yes
	The MIC method in [32]	75.00	279.7	0.41	99.21	79.34	Yes
	The original PIO method	75.00	279.7	0.30	99.21	92.19	Yes
Case 4	The proposed HPIO method	34.86	172.1	0.30	99.55	90.65	Yes
	The DPSO method in [29]	33.82	172.1	0.50	99.55	75.14	Yes
	The MFA method in [30]	37.59	155.2	0.20	89.78	83.68	No
	The OD method in [21]	34.62	172.3	0.40	99.67	83.48	Yes
	The S-Jaya method in [31]	34.10	172.3	0.35	99.67	89.59	Yes
	The MIC method in [32]	34.61	172.3	0.43	99.67	77.17	Yes
	The original PIO method	34.78	172.1	0.30	99.55	87.87	Yes

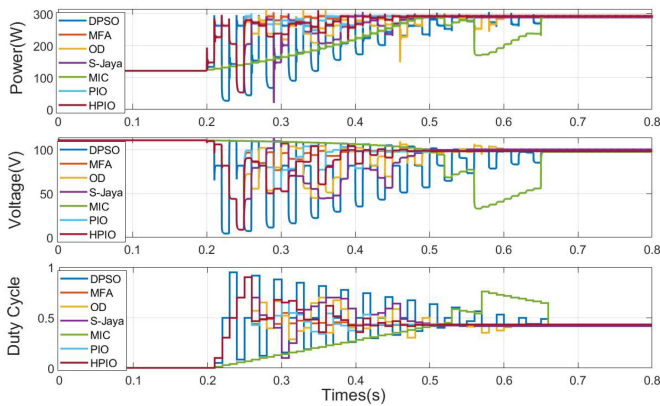


Fig. 8. Output waveforms during the tracking process in Case 2.

3) *Case 3*: It can be seen from Fig. 9 that the proposed HPIO and S-Jaya method complete the tracking within 0.3 and 0.35 s, respectively, and the static tracking efficiency reaches 99.38%. The DPSO, MFA and OD methods complete tracking within 0.42, 0.2, and 0.4 s, respectively. These three MPPT methods finally achieve the same static tracking efficiency of 99.35%. The MIC and original PIO method complete the tracking within 0.41 and 0.30 s, respectively, and their static tracking efficiency reach 99.21%. In this case, the MFA method shows the highest dynamic tracking efficiency of 94.67%, the HPIO method is second only with 92.87%, the dynamic tracking efficiency of MPPT methods except DPSO, OD, and MIC reach more than 90%. The proposed HPIO method still shows the tracking speed and dynamic tracking efficiency

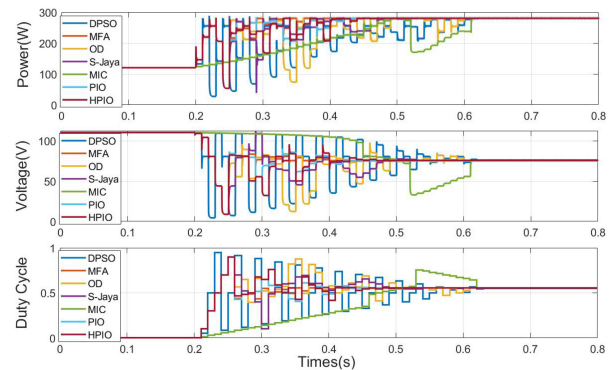


Fig. 9. Output waveforms during the tracking process in Case 3.

second only to the MFA method and the highest static tracking efficiency among the six MPPT methods.

4) *Case 4*: It can be observed from Fig. 10 that the proposed HPIO and original PIO methods complete tracking within 0.3 s, and the static tracking efficiency reaches 99.55%. The DPSO method still does not converge within 0.50 s, and the maximum number of samplings is reached at this time so that it ends tracking and outputs the optimal point. The MFA method only needs 0.2 s to complete the tracking; however, due to the overly fast convergence, the tracked position deviates from the GMPP, the static tracking efficiency is only 89.78%; thus, it fails to track the GMPP. The OD, S-Jaya, and MIC method complete the tracking within 0.4, 0.35, and 0.43 s, respectively, and the static efficiency reaches 99.67%. The proposed HPIO method shows the highest dynamic tracking efficiency of 90.65%; while the dynamic tracking efficiency of other

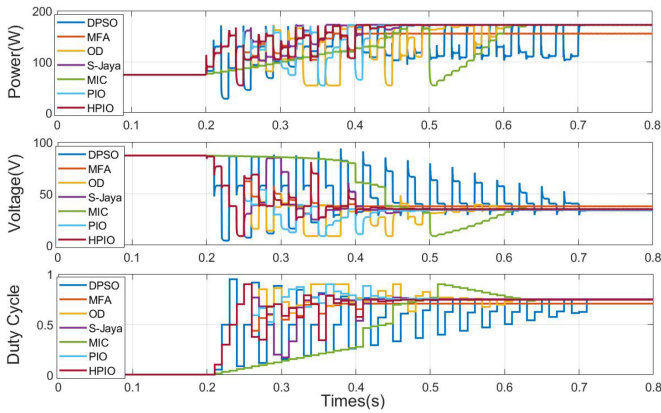


Fig. 10. Output waveforms during the tracking process in Case 4.

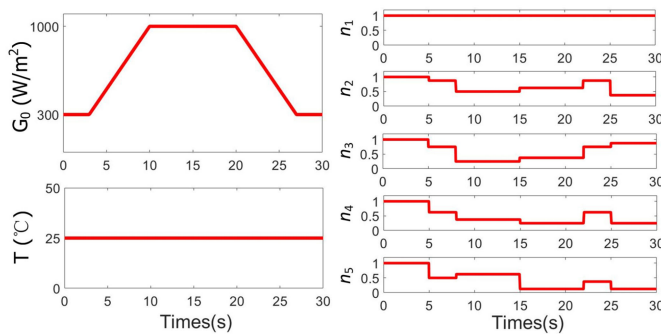


Fig. 11. Test profiles for dynamic tracking test.

MPPT methods fail to reach 90%. In Case 4, the MFA method fails to realize MPPT, again indicating that its shadow tracking ability is also lacking.

- 5) *Dynamic tracking test*: In order to verify the practicability of the MPPT design based on the two modes proposed in this article for long-term tracking, dynamic tracking tests are carried out on the seven MPPT methods under the simulation environment of dynamic changes in irradiance and continuous switching of PSCs. The seven MPPT methods are tested using the MPPT framework based on two modes. Based on the EN50530 standard, a 30%–100% ramp with a slope of 100 W/m^2 and a dwell time of 10 s is selected as the irradiance curve. It should be noted that the percentage specification of irradiance is related to STC, and 100% corresponds to 1000 W/m^2 at 25°C . The test profiles, including the selected irradiance curve and the percentage n_i of the irradiance received by each PV panel in real time, are shown in Fig. 11. And Fig. 12 shows the power waveforms of seven MPPT methods in the current test environment. It can be seen that all MPPT methods still keep track of GMPP during the whole process of changing environmental conditions. In the proposed MPPT framework based on two modes, the intelligent MPPT algorithm is restarted to find a new GMPP so that effectively dealing with PSC switching.
- 6) *Summary*: Based on the analysis of the abovementioned four cases, it can be seen that the proposed HPIO method

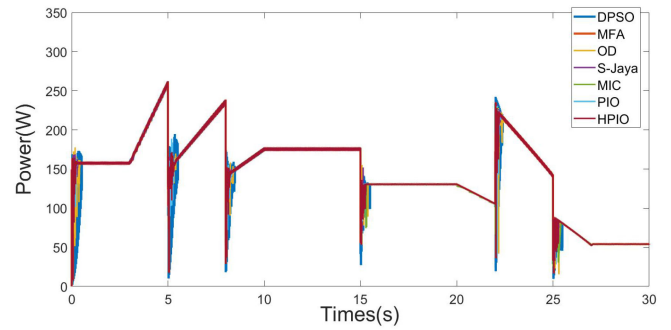


Fig. 12. Power waveforms during the dynamic tracking test.

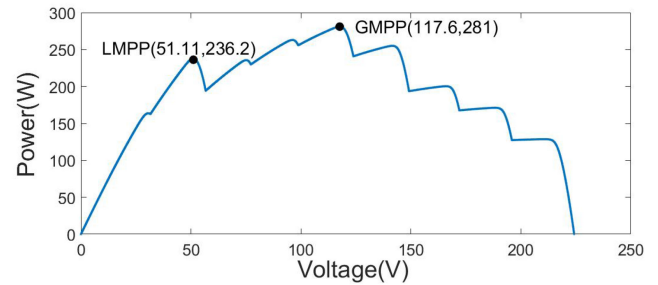


Fig. 13. P-V characteristic curve under complex PSC with multiple clusters.

still has perfect shadow tracking ability and high static and dynamic tracking efficiency in a relatively short tracking time, and has the best overall performance among the seven MPPT methods. It indicates that the proposed HPIO method has superior performance in dealing with complex PSCs.

Through the change of duty cycle and voltage waveform of the proposed HPIO method, it can be seen that from the initial distribution to the end of the first stage of optimization, the change trend of duty cycle and voltage is relatively gentle due to the stratified movement, and will not gather to the current global optimal power point too quickly, thus realizing the precise search for various locations within the initial distribution range during the process of multiple iterations. In the second stage of optimization, due to the reduction of population size, the tracking time is very short. During this period, the duty cycle and voltage fluctuate around the global optimal power point to ensure that GMPP could be found.

E. Complex PSC With Multiple Clusters

Kermadi *et al.* [13] discussed that complex PSC may form multiple clusters, and each cluster has its own middle peak (MHP). The P-V curve with multiple MHP brings difficulties to tracking MPP. In order to verify that the proposed HPIO method is still valid under PSC with multiple clusters, the following simulation results are given. The P-V characteristic curve of the PSC selected for the simulation is shown in Fig. 13. It can be seen that the curve has two MHPs, and GMPP is at the middle of the curve. In this curve, V_{MPP} is 117.6 V, and P_{MPP} is 281.0 W.

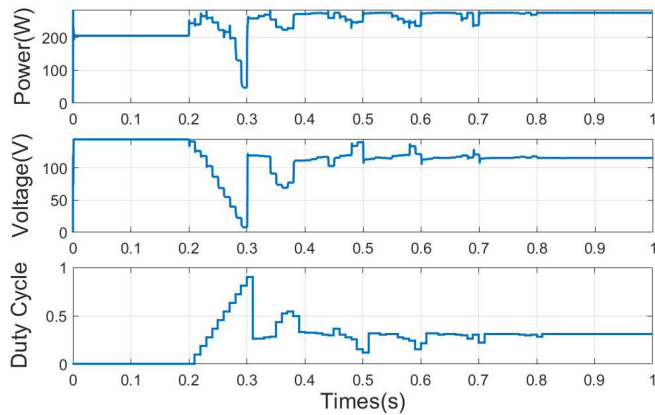


Fig. 14. Output waveforms under PSC with multiple clusters.

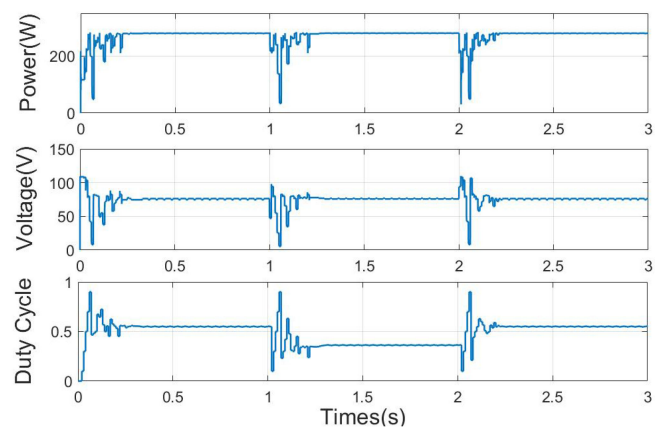


Fig. 15. Output waveforms during the load-variation test.

Fig. 14 shows the output waveforms of the proposed HPIO method in the current shading pattern. It can be observed from Fig. 14 that the proposed HPIO complete tracking within 0.6 s, V_m is 115.3 V, and P_m is 275.0 W. The static tracking efficiency reaches 97.86%, and the dynamic tracking efficiency within 0.8 s reaches 92.65%. Therefore, it can be concluded that the proposed HPIO method can still successfully track GMPP under complex PSC with multiple clusters.

F. Load Changes Under PSCs

In practical applications, in addition to constantly changing irradiance conditions, load changes are also important external conditions that affect the dynamic operation of the PV system. In order to verify the effectiveness of the proposed MPPT design based on the two modes in response to load changes, load-varying tests are carried out on the proposed HPIO method.

In this test, select Case 3, which is given in Table I and Fig. 3, as the PSC. V_{MPP} is 76.38 V, and P_{MPP} is 281.9 W. Fig. 15 shows the output waveforms of the proposed HPIO method during the load-variation test. The initial load value is $R = 100 \Omega$. When $t = 0$ s, the MPPT method is started and GMPP is successfully traced. When $t = 1$ s, the load becomes $R = 50 \Omega$; therefore, the controller detects the power fluctuation caused by the load change, and restarts the MPPT method. When $t = 2$ s,

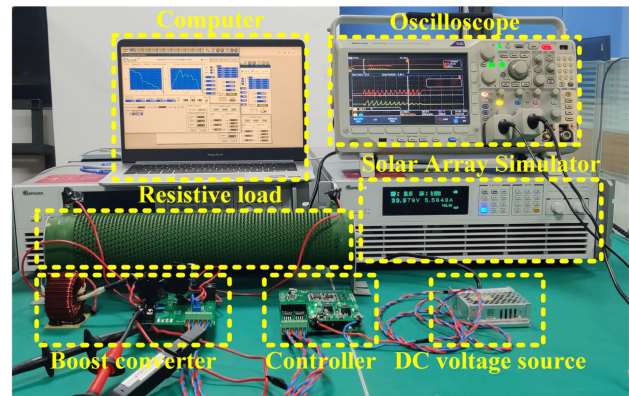


Fig. 16. Composition of the experimental platform.

TABLE VII
PARAMETERS OF CIRCUIT COMPONENTS

Specification	Parameter
Input Voltage at MPP (V_{in})	84.2 V
Output Power of PV array at MPP (P_{out})	507.0 W
Switching Frequency (f_s)	20 kHz
L	5 mH
C_{in}	100 μ F
C_{out}	47 μ F

the load becomes $R = 100 \Omega$; therefore, the MPPT method is restarted again. According to the results shown in Fig. 15, it can be seen that the load change conditions will not reduce the tracking performance of the proposed MPPT design based on two modes.

V. EXPERIMENTAL RESULTS AND DISCUSSIONS

The experimental platform consists of a solar array simulator (Chroma A62028), a boost converter, a load, a control circuit, an oscilloscope (Tektronix MDO 3024), as shown in Fig. 16. The parameters are shown in Table VII. The proposed HPIO MPPT method and the other three MPPT methods for comparison are implemented based on MCU RT1052 with 528 MHz clock, 32 MB flash memory, 1 MB SRAM, and ADC chip AD7606 with the resolution of 16 bits. Four cases given in Fig. 3 are loaded into the solar array simulator to obtain the P-V and I-V curves under the four cases, as shown in Fig. 17.

The input voltage and inductor current of the boost converter pass through the voltage-voltage and current-voltage conversion circuit, and after being sampled by AD7606, they are transmitted to the program that implements the MPPT method. The MPPT methods adjust the position of the tracking point by outputting a duty cycle to the boost converter, thereby achieving MPPT technology. Due to the need to consider the response speed of the circuit in the steady state during each sampling process, the sampling time, which is from the controller output duty cycle to the collection of the voltage and current values, is set to 0.055 s to meet the technical requirements of MPPT. In this section, three AI-based MPPT methods, i.e., DPSO, MFA, and OD, are selected to compare the tracking performance with the proposed HPIO method in the same experimental environment.

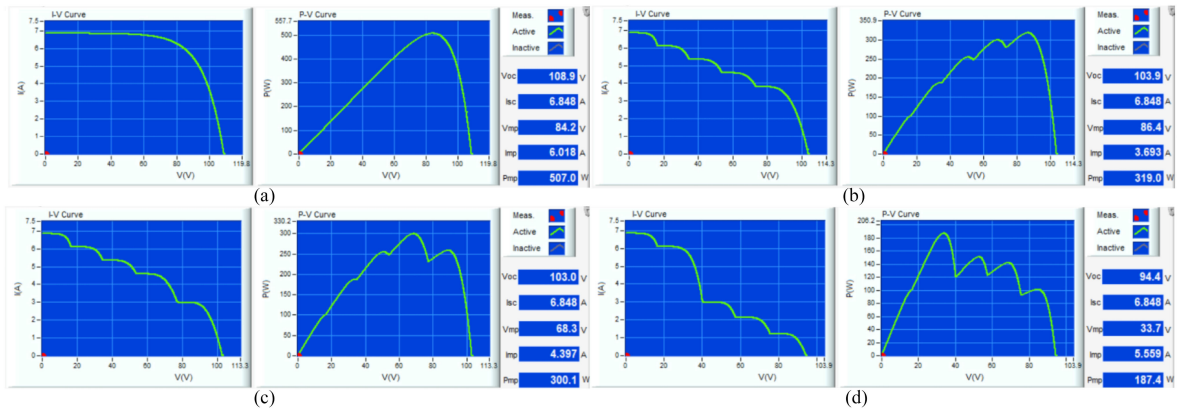


Fig. 17. P-V and I-V curves under four cases in experiment. (a) Case 1. (b) Case 2. (c) Case 3. (d) Case 4.

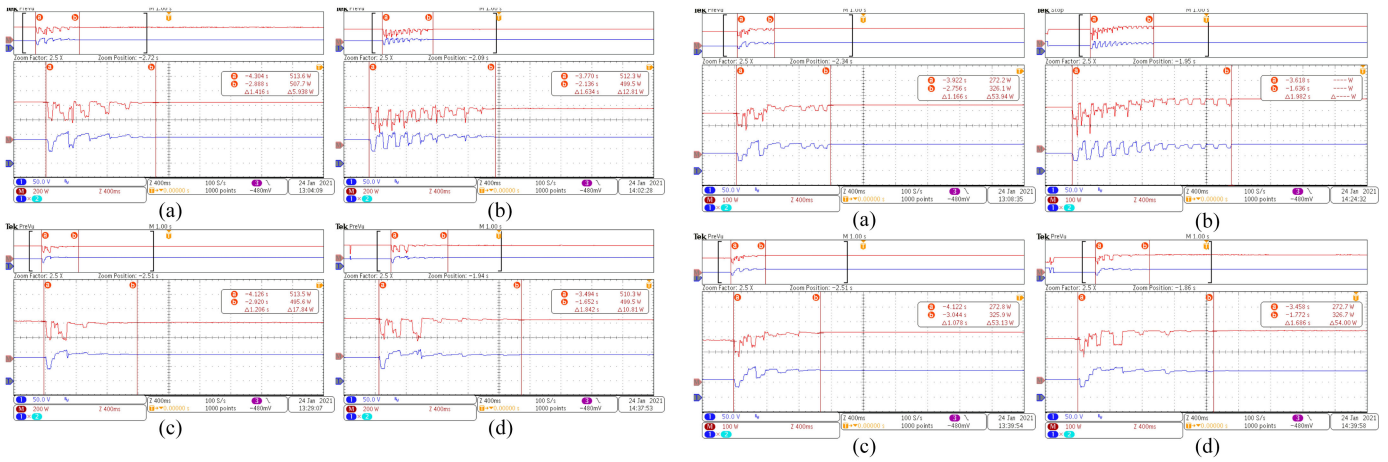


Fig. 18. Output power and output voltage waveforms under Case 1. (a) Proposed HPIO method. (b) DPSO method. (c) MFA method. (d) OD method.

Fig. 19. Output power and output voltage waveforms under Case 2. (a) Proposed HPIO method. (b) DPSO method. (c) MFA method. (d) OD method.

Considering that the S-Jaya method exhibits weak tracking performance, the MIC method requires additional parameters of the PV array so that it causes inconvenience to the practical application, and the original PIO method is the prototype of the HPIO method, these three methods are not selected as the comparison method. In the experiment, the duty cycle range of all MPPT methods is set at [0.1, 0.70]. The other parameters of the four MPPT methods in the experiment are the same as the other parameters of the simulation research.

- 1) *Case 1*: Fig. 18 shows the output power and output voltage waveforms of the PV system. For the proposed HPIO method, it takes 1.416 s to complete the MPPT process. After the power stabilizes, the measured tracking power is 500.7 W, and the efficiency reaches 98.76%. For the DPSO method, MFA method and OD method, the tracking time reaches 1.634, 1.206, and 1.842 s, respectively, and the tracking efficiency also reaches 97.75%, 96.79%, and 97.73%. Compared with other three MPPT methods, the proposed HPIO method has a higher tracking efficiency. Although the MFA method has the fastest tracking speed, its tracking efficiency is 1.97% lower than that of the proposed HPIO method.

- 2) *Case 2*: As observed from Fig. 19, for the proposed HPIO method, it takes 1.166 s to complete the MPPT, and the tracking efficiency reaches 99.81%. For the DPSO method, MFA method and OD method, the tracking time is 1.982, 1.078, and 1.686 s, respectively, and the tracking efficiency reaches 99.75%, 99.69%, and 99.72%. In this case, the four MPPT methods successfully track to the power point near GMPP. The proposed HPIO method and MFA method have significantly faster tracking speeds compared with the other two methods.
- 3) *Case 3*: As seen from Fig. 20, for the proposed HPIO method, it takes 1.150 s to complete the MPPT process, and the tracking efficiency reaches 99.80%. For the DPSO method, MFA method and OD method, the tracking time is 2.114, 0.834, and 1.738 s, respectively, and the tracking efficiency reaches 99.83%, 93.74%, and 99.87% as well. The MFA method can only track to the power point of 7.82% Voc away from GMPP due to the fast convergence, which leads to the failure of tracking GMPP. Moreover, due to the slow convergence of the DPSO method, the MPPT ends when the maximum number of samples is reached.

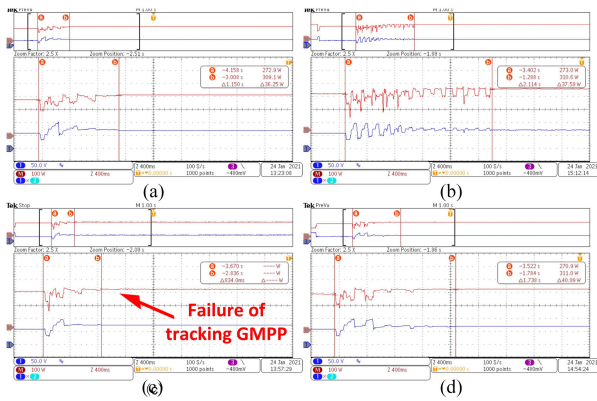


Fig. 20. Output power and output voltage waveforms under Case 3. (a) Proposed HPIO method. (b) DPSO method. (c) MFA method. (d) OD method.

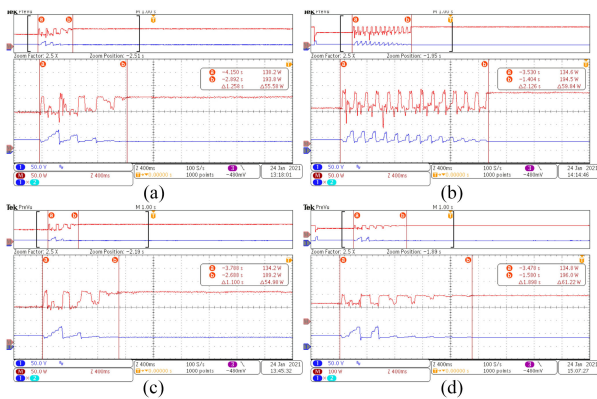


Fig. 21. Output power and output voltage waveforms under Case 4. (a) Proposed HPIO method. (b) DPSO method. (c) MFA method. (d) OD method.

- 4) *Case 4:* As observed from Fig. 21, for the proposed HPIO method, it takes 1.258 s to complete the MPPT process with the tracking efficiency of 98.72%. For the DPSO method, MFA method and OD-PSO method, the tracking time is 2.126, 1.100, and 1.898 s, respectively, and the tracking efficiency reaches 98.72%, 98.19%, and 98.88% too. Similarly, the proposed HPIO and MFA have significantly faster tracking speed than the other two MPPT methods. MFA has the fastest tracking speed, but its tracking efficiency is slightly lower among the four MPPT methods. Due to the slow convergence, the DPSO method completes the MPPT with the slowest tracking speed.
- 5) *Summary:* It can be seen that by comprehensively considering multiple indicators of tracking success rate, tracking efficiency, and tracking speed, the proposed HPIO method shows better tracking performance than the DPSO method, the MFA method, and the OD method. The proposed HPIO method solves the problem that the rapid convergence of the MFA method may fall into LMPP, and also solves the problem that the convergence speed of the DPSO method and the OD-PSO method is not fast enough for foreseeable practical applications. In addition, the

tracking performance of the four MPPT methods tested under the four cases in the experiment is similar to the results obtained by the simulation, which further verifies the accuracy of this article.

As the attention to the research on PV systems continues to increase, the need to solve the problem of dust accumulation has gradually emerged. The research in [33] shows that dust accumulation will cause a decrease in voltage and current, while the drop in the open voltage can be ignored and the reduction in the output current is the main reason for the power drop. It will also reduce the inertia against the variation in the P-V and I-V characteristic curves, thus adding certain difficulties to the realization of MPPT technology. In a well-ventilated installation environment, the degree of dust accumulation on each PV panel is the same, which will not directly lead to the production of PSC. However, in the actual production and operation process, the degree of dust accumulation on each panel may be different due to the influence of the terrain around the installation environment. At this time, even if the PV system receives uniform illumination, there may be multiple power extreme points on the actual P-V characteristic curve. The existing MPPT method that can track GMPP under PSCs can also cope with the problem of dust accumulation to a certain extent.

VI. CONCLUSION

In this article, a hierarchical pigeon-inspired optimization method was proposed for efficient and fast maximum power point tracking of PV system. In order to strengthen the global search capability, a hierarchical network in the pigeon flock was constructed to revise the map and compass operator of the original PIO algorithm to ensure superior tracking efficiency and tracking success rate. At the same time, the landmark operator can also ensure fast convergence to save tracking time. On this basis, a tracking mechanism that switches between “Intelligent Mode” and “Disturbance Mode” was proposed. With these two modes, not only can the problem of searching for GMPP under PSCs be effectively solved, but also long-term efficient dynamic tracking can be maintained. Comparative simulated results with 56 PSCs and experimental results under four typical irradiation cases verify the excellent tracking performance of the proposed HPIO method as compared with typical existing advanced MPPT techniques. Simulated results of dynamic tracking test also verify the effectiveness of the proposed MPPT framework based on two modes for practical applications. The proposed HPIO method effectively achieves a good balance between the two indicators of tracking efficiency and tracking speed in MPPT. To increase the practical application of the method further, it is important to carry out more research to deal with dust accumulation in future work too.

REFERENCES

- [1] J. Ahmed and Z. Salam, “An accurate method for MPPT to detect the partial shading occurrence in a PV system,” *IEEE Trans. Ind. Informat.*, vol. 13, no. 5, pp. 2151–2161, Oct. 2017.
- [2] N. Femia, G. Petrone, G. Spagnuolo, and M. Vitelli, “Optimization of perturb and observe maximum power point tracking method,” *IEEE Trans. Power Electron.*, vol. 20, no. 4, pp. 963–973, Jul. 2005.

- [3] Chia-Hung Lin *et al.*, "Maximum photovoltaic power tracking for the PV array using the fractional-order incremental conductance method," *Appl. Energy*, vol. 88, no. 12, pp. 4840–4847, 2011.
- [4] E. Koutroulis, K. Kalaitzakis, and N. C. Voulgaris, "Development of a microcontroller-based, photovoltaic maximum power point tracking control system," *IEEE Trans. Power Electron.*, vol. 16, no. 1, pp. 46–54, Jan. 2001.
- [5] B. N. Alajmi, K. H. Ahmed, S. J. Finney, and B. W. Williams, "Fuzzy-logic-control approach of a modified hill-climbing method for maximum power point in microgrid standalone photovoltaic system," *IEEE Trans. Power Electron.*, vol. 26, no. 4, pp. 1022–1030, Apr. 2011.
- [6] Syafaruddin *et al.*, "Artificial neural network-polar coordinated fuzzy controller-based maximum power point tracking control under partially shaded conditions," *IET Renewable Power Gener.*, vol. 3, no. 2, pp. 239–253, 2009.
- [7] B. Lin, L. Wang, and Q. Wu, "Maximum power point scanning for PV systems under various partial shading conditions," *IEEE Trans. Sustain. Energy*, vol. 11, no. 4, pp. 2556–2566, Oct. 2020.
- [8] M. Kermadi, Z. Salam, J. Ahmed, and E. M. Berkouk, "A high-performance global maximum power point tracker of PV system for rapidly changing partial shading conditions," *IEEE Trans. Ind. Electron.*, vol. 68, no. 3, pp. 2236–2245, Mar. 2021.
- [9] J. H. Holland, *Adaptation in Natural and Artificial Systems: An Introductory Analysis With Applications to Biology, Control, and Artificial Intelligence*. Cambridge, MA, USA: MIT Press, 1992.
- [10] R. Storn and K. Price, "Differential evolution – a simple and efficient heuristic for global optimization over continuous spaces," *J. Glob. Optim.*, vol. 11, pp. 341–359, 1997.
- [11] A. Messai *et al.*, "Maximum power point tracking using a GA optimized fuzzy logic controller and its FPGA implementation," *Sol. Energy*, vol. 85, pp. 265–277, 2011.
- [12] K. S. Tey *et al.*, "Improved differential evolution-based MPPT algorithm using SEPIC for PV systems under partial shading conditions and load variation," *IEEE Trans. Ind. Informat.*, vol. 14, no. 10, pp. 4322–4333, Oct. 2018.
- [13] M. Kermadi, Z. Salam, J. Ahmed, and E. M. Berkouk, "An effective hybrid maximum power point tracker of photovoltaic arrays for complex partial shading conditions," *IEEE Trans. Ind. Electron.*, vol. 66, no. 9, pp. 6990–7000, Sep. 2019.
- [14] M. Seyedmahmoudian, T. K. Soon, B. Horan, A. Ghandhari, S. Mekhilef, and A. Stojcevski, "New ARMO-based MPPT technique to minimize tracking time and fluctuation at output of PV systems under rapidly changing shading conditions," *IEEE Trans. Ind. Informat.*, to be published, doi: [10.1109/TII.2019.2495066](https://doi.org/10.1109/TII.2019.2495066).
- [15] N. Priyadarshi, S. Padmanaban, J. B. Holm-Nielsen, F. Blaabjerg, and M. S. Bhaskar, "An experimental estimation of hybrid ANFIS-PSO-based MPPT for PV grid integration under fluctuating sun irradiance," *IEEE Syst. J.*, vol. 14, no. 1, pp. 1218–1229, Mar. 2020.
- [16] N. Singh, K. K. Gupta, S. K. Jain, N. K. Dewangan, and P. Bhatnagar, "A flying squirrel search optimization for MPPT under partial shaded photovoltaic system," *IEEE J. Emerg. Sel. Topics Power Electron.*, vol. 9, no. 4, pp. 4963–4978, Aug. 2021.
- [17] D. S. Pillai, J. P. Ram, A. M. Y. M. Ghias, M. A. Mahmud, and N. Rajasekar, "An accurate, shade detection-based hybrid maximum power point tracking approach for PV systems," *IEEE Trans. Power Electron.*, vol. 35, no. 6, pp. 6594–6608, Jun. 2020.
- [18] Y. -P. Huang, M. -Y. Huang, and C. -E. Ye, "A fusion firefly algorithm with simplified propagation for photovoltaic MPPT under partial shading conditions," *IEEE Trans. Sustain. Energy*, vol. 11, no. 4, pp. 2641–2652, Oct. 2020.
- [19] S. Makhloufi and S. Mekhilef, "Logarithmic PSO based global/local maximum power point tracker for partially shaded photovoltaic systems," *IEEE J. Emerg. Sel. Topics Power Electron.*, to be published, doi: [10.1109/JESTPE.2021.3073058](https://doi.org/10.1109/JESTPE.2021.3073058).
- [20] I. Shams, S. Mekhilef, and K. S. Tey, "Maximum power point tracking using modified butterfly optimization algorithm for partial shading, uniform shading, and fast varying load conditions," *IEEE Trans. Power Electron.*, vol. 36, no. 5, pp. 5569–5581, May 2021.
- [21] H. Li, D. Yang, W. Su, J. Lü, and X. Yu, "An overall distribution particle swarm optimization MPPT algorithm for photovoltaic system under partial shading," *IEEE Trans. Ind. Electron.*, vol. 66, no. 1, pp. 265–275, Jan. 2019.
- [22] H. Duan and P. Qiao, "Pigeon-inspired optimization: A new swarm intelligence optimizer for air robot path planning," *Int. J. Intell. Comput. Cybern.*, vol. 7, no. 1, pp. 24–37, 2014.
- [23] Daifeng Zhang and Haibin Duan, "Social-class pigeon-inspired optimization and time stamp segmentation for multi-UAV cooperative path planning," *Neurocomputing*, vol. 313, pp. 229–246, 2018.
- [24] Z. JIA, "A type of collective detection scheme with improved pigeon-inspired optimization," *Int. J. Intell. Comput. Cybern.*, vol. 9, no. 1, pp. 105–123, 2016.
- [25] Kashif Ishaque *et al.*, "Modeling and simulation of photovoltaic (PV) system during partial shading based on a two-diode model," *Simul. Model. Pract. Theory*, vol. 19, no. 7, pp. 1613–1626, 2011.
- [26] Tim Guilford *et al.*, "Positional entropy during pigeon homing II: Navigational interpretation of bayesian latent state models," *J. Theor. Biol.*, vol. 227, no. 1, pp. 25–38, 2004.
- [27] M. Nagy *et al.*, "Hierarchical group dynamics in pigeon flocks," *Nature*, vol. 464, pp. 890–893, 2010.
- [28] M. Nagy *et al.*, "Context-dependent hierarchies in pigeons," *Proc. Nat. Acad. Sci.*, vol. 110, no. 32, pp. 13049–13054, Aug. 2013.
- [29] K. Ishaque and Z. Salam, "A deterministic particle swarm optimization maximum power point tracker for photovoltaic system under partial shading condition," *IEEE Trans. Ind. Electron.*, vol. 60, no. 8, pp. 3195–3206, Aug. 2013.
- [30] D. F. Teshome, C. H. Lee, Y. W. Lin, and K. L. Lian, "A modified firefly algorithm for photovoltaic maximum power point tracking control under partial shading," *IEEE J. Emerg. Sel. Topics Power Electron.*, vol. 5, no. 2, pp. 661–671, Jun. 2017.
- [31] C. Huang, L. Wang, R. S. Yeung, Z. Zhang, H. S. Chung, and A. Bensoussan, "A prediction model-guided jaya algorithm for the PV system maximum power point tracking," *IEEE Trans. Sustain. Energy*, vol. 9, no. 1, pp. 45–55, Jan. 2018.
- [32] M. A. Ghasemi, H. M. Foroushani, and M. Parniani, "Partial shading detection and smooth maximum power point tracking of PV arrays under PSC," *IEEE Trans. Power Electron.*, vol. 31, no. 9, pp. 6281–6292, Sep. 2016.
- [33] A. Gholami, M. Ameri, M. Zandi, R. G. Ghoachani, S. Eslami, and S. Pierfederici, "Photovoltaic potential assessment and dust impacts on photovoltaic systems in Iran: Review paper," *IEEE J. Photovolt.*, vol. 10, no. 3, pp. 824–837, May 2020.



Zhuoli Zhao (Member, IEEE) received the Ph.D. degree in electrical engineering from the South China University of Technology, Guangzhou, China, in 2017.

From October 2014 to December 2015, he was a Joint Ph.D. Student (Sponsored Researcher) with the Control and Power Research Group, Department of Electrical and Electronic Engineering, Imperial College London, London, U.K. He was a Research Associate with the Smart Grid Research Laboratory, Electric Power Research Institute, China Southern Power Grid, Guangzhou, from 2017 to 2018. He is currently an Associate Professor with the School of Automation, Guangdong University of Technology, Guangzhou. His research interests include microgrid control and energy management, power electronic converters, smart grids, and distributed generation systems.

Prof. Zhao is an Active Reviewer for the IEEE TRANSACTIONS ON SMART GRID, IEEE TRANSACTIONS ON POWER ELECTRONICS, IEEE TRANSACTIONS ON SUSTAINABLE ENERGY, IEEE TRANSACTIONS ON INDUSTRIAL ELECTRONICS, and *Applied Energy*.



Mingyu Zhang is currently working toward the bachelor's degree in electrical engineering with the School of Automation, Guangdong University of Technology, Guangzhou, China.

His research interests include power electronic converters and smart grids.



Zehan Zhang is currently working toward the bachelor's degree in electrical engineering with the School of Automation, Guangdong University of Technology, Guangzhou, China.

His research interests include embedded control and energy management in power electronic converters and smart grids.



Yuewu Wang received the B.S. degree in instrument science and technology from Xi'an Jiaotong University, Xi'an, China, in 2006, the M.S. degree in electrical engineering from Guangxi University, Nanning, China, in 2010, and the Ph.D. degree in electrical engineering from the South China University of Technology, Guangzhou, China, in 2017.

From 2017 to 2020, he was a Software Engineer with Shenzhen INVT Electric Co., Ltd., Shenzhen, China. In 2020, he was with the

School of Electric and Information Engineering, Guangxi University of Science and Technology, Liuzhou, China, where he is currently a Lecturer. His current research interests include pulse width modulation techniques, dc-dc converters, and grid-connected inverters.



Runting Cheng received the B.Eng. degree in electrical engineering and automation from Northeast Forestry University, Harbin, China, in 2018, and the M.S. degree in electrical engineering from the Guangdong University of Technology, Guangzhou, China, in 2021.

She is currently a Research Assistant with the South China University of Technology, Guangzhou. Her research interests include distribution network dispatching and distributed generation systems.



Juntao Guo received the B.E. degree in electrical engineering and automation in 2019 from the Guangdong University of Technology, Guangzhou, China, where he is currently working toward the master's degree in electrical engineering with the School of Automation.

His research interests include microgrid control and energy management.



Ping Yang (Member, IEEE) received the Ph.D. degree in automatic control from the South China University of Technology, Guangzhou, China, in 1998.

She is currently a Professor with the School of Electric Power Engineering, South China University of Technology, and the Director of Guangdong Key Laboratory of Clean Energy Technology, South China University of Technology. Her current research interests include smart microgrid and electricity market.



Chun Sing Lai (Senior Member, IEEE) received the B.Eng. (first class hon.) degree in electrical and electronic engineering from Brunel University London, London, U.K., in 2013, and the D.Phil. degree in engineering science from the University of Oxford, Oxford, U.K., in 2019.

He is currently a Lecturer with the Department of Electronic and Electrical Engineering, Brunel University London. From 2018 to 2020, he was an U.K. Engineering and Physical Sciences Research Council Research Fellow with the School of Civil Engineering, University of Leeds, Leeds, U.K. His current research interests include power system optimization and data analytics.

Dr. Lai was the Publications Co-Chair for both 2020 and 2021 IEEE International Smart Cities Conferences. He is the Vice-Chair of the IEEE Smart Cities Publications Committee and Associate Editor for IET Energy Conversion and Economics. He is the Working Group Chair for IEEE P2814 Standard, and the Chair of the IEEE SMC Intelligent Power and Energy Systems Technical Committee. He is an *IET Member and a Chartered Engineer*.



Peng Li received the B.Sc., M.Sc., and Ph.D. degrees from the South China University of Technology, Guangzhou, China, in 1993, 1995, and 2002, respectively, and the Ph.D. degree from the Technical University of Braunschweig, Braunschweig, Germany, in 2004, all in electrical engineering.

He is currently a Professor-level Senior Engineer of the Digital Grid Research Institute of China Southern Power Grid, Guangzhou. His current research interests include technology research and management of smart grid and digital grid.



Loi Lei Lai (Life Fellow, IEEE) received the B.Sc. (first class hon.), Ph.D., and D.Sc. degrees in electrical and electronic engineering from the University of Aston, Birmingham, U.K., and City, University of London, London, U.K., in 1980, 1984, and 2005, respectively.

He is currently a University Distinguished Professor with the Guangdong University of Technology, Guangzhou, China. He was a Pao Yue Kong Chair Professor with Zhejiang University, Hangzhou, China, and the Professor and Chair of Electrical Engineering with City, University of London. His current research interests include smart cities and smart grid.

Prof. Lai was the recipient of the IEEE Third Millennium Medal, IEEE Power and Energy Society (IEEE/PES) UKRI Power Chapter Outstanding Engineer Award in 2000, IEEE/PES Energy Development and Power Generation Committee Prize Paper in 2006 and 2009, IEEE/SMCS Outstanding Contribution Award in 2013 and 2014, Most Active Technical Committee Award in 2016, and his research team has received a Best Paper Award in the IEEE International Smart Cities Conference in October 2020. He is an Associate Editor for the IEEE TRANSACTIONS ON SYSTEMS, MAN, AND CYBERNETICS: SYSTEMS, Editor-in-Chief for the IEEE SMART CITIES NEWSLETTER, a Member of the IEEE Smart Cities Steering Committee, and the Chair of the IEEE Systems, Man, and Cybernetics Society (IEEE/SMCS) Standards Committee. He was a Member of the IEEE Smart Grid Steering Committee; the Director of Research and Development Center, State Grid Energy Research Institute, China; a Vice President for Membership and Student Activities with IEEE/SMCS; and a Fellow Committee Evaluator for the IEEE Industrial Electronics Society. He is a Fellow of IET.